

RSC Advances



This is an *Accepted Manuscript*, which has been through the Royal Society of Chemistry peer review process and has been accepted for publication.

Accepted Manuscripts are published online shortly after acceptance, before technical editing, formatting and proof reading. Using this free service, authors can make their results available to the community, in citable form, before we publish the edited article. This *Accepted Manuscript* will be replaced by the edited, formatted and paginated article as soon as this is available.

You can find more information about *Accepted Manuscripts* in the [Information for Authors](#).

Please note that technical editing may introduce minor changes to the text and/or graphics, which may alter content. The journal's standard [Terms & Conditions](#) and the [Ethical guidelines](#) still apply. In no event shall the Royal Society of Chemistry be held responsible for any errors or omissions in this *Accepted Manuscript* or any consequences arising from the use of any information it contains.

1 **Internal and External Factors affecting the Stability of Glycerol Monostearate Structured**
2 **Emulsions**

3

4 Fan C. Wang and Alejandro G. Marangoni*

5

6 Department of Food Science, University of Guelph

7 50 Stone Road W, Guelph, ON, Canada. N1G 2W1

8 Corresponding author e-mail: amarango@uoguelph.ca

9

10 **Abstract**

11 Monoglyceride (MG) structured emulsions have been developed for use in diverse food and
12 cosmetic applications. However, these MG-structured emulsions undergo a polymorphic
13 transformation from the α -gel phase to the coagel phase, resulting in emulsion destabilization
14 and water syneresis. In this study, the stability of emulsions containing 60-70% (w/w) water
15 structured with 5% (w/w) of a blend of the emulsifier glycerol monostearate (GMS) and co-
16 emulsifier sodium stearyl lactylate (SSL), was assessed. The internal factors examined were
17 concentrations of co-emulsifier and the addition of the polysaccharide xanthan gum. External
18 factors examined included cooling rate and applied shear. The methods used to study the
19 polymorphic transition were differential scanning calorimetry, X-ray diffraction, and pulsed
20 proton nuclear magnetic resonance. In this work, the sub- α Coagel Index was successfully used
21 to characterize the degree of coagel formation in MG-structured emulsions. Results showed that
22 the stability of the α -gel phase was improved by using 1:9 w/w SSL: GMS ratios and by adding

23 0.1% xanthan gum. Slow cooling rates without shear could also increase the stability of the α -gel
24 phase in the structured emulsion system.

25

26 **1. Introduction**

27 Monoglycerides (MGs) are lipid molecules that have one fatty acyl chain attached to a
28 glycerol backbone, and are thus amphiphilic. They self-assemble both in water and oil into
29 several types of mesophases, depending on temperature and concentration¹, and are used
30 extensively in food and personal care products.¹ Our group developed a MG-structured oil-in-
31 water (o/w) emulsion that contains 3-5 % (w/w) of saturated MGs, 0.15–0.25 % (w/w) of co-
32 emulsifier, 10-70 % (w/w) of oil, and 20-60 % (w/w) of water.²⁻⁴ This structured emulsion has
33 been shown to function as a shortening that has no *trans* fat and low in saturated fat.^{3,4} The
34 physical properties of these MG-structured emulsions can be tailored to replace shortening in
35 most bakery products such as cookies⁵, breads⁶, and laminated puff pastries⁷.

36 The structural and rheological properties of MG-structured emulsions have been studied
37 and the lamellar phase has been found to be the optimal structure for a spreadable emulsion.⁴
38 Upon homogenization, the MGs and co-emulsifiers self-assemble into hydrated lamellar
39 structures and form a fat-like gel network, in which oil droplets are surrounded by alternating
40 MG-bilayers and water.^{3,4,8-10}

41 However, MG-structured emulsions are prone to phase separation and water syneresis
42 can be observed after four weeks of storage at room temperature. The emulsion destabilization is
43 mainly caused by a polymorphic transformation of the MGs.^{1,11-14} In order to increase the water
44 swelling capacity of the MG-bilayers, which could improve the stability of the MG-structured
45 emulsion, the nature and dynamics of the polymorphic behavior of MG-water systems must be

46 better understood.

47 The polymorphic behavior of glycerol monostearate (GMS) in water has been well
48 characterized in previous work. When heating a GMS-water mixture above its Krafft
49 temperature (T_k), GMS molecules self-assemble into an L_α liquid crystalline phase.^{11,13,14} Further
50 heating of the system above 80°C leads to the formation of cubic phases.^{10,14,15} Upon cooling the
51 L_α liquid crystalline phase below T_k , the hydrocarbon chains of the GMS lose mobility and
52 transform into an L_β phase (α -gel phase), in which thick layers of water are retained between the
53 MG bilayers. The α -gel phase undergoes a thermally reversible phase transition to the sub- α -gel
54 phase when the temperature drops below 13°C.¹⁶ However, both the sub- α -gel phase and the α -
55 gel phase are thermodynamically unstable and will gradually crystallize into a more densely
56 packed L_β phase (the coagel phase), accompanied by a release of water from the bilayer
57 structures.^{1,11,13,17}

58 The polymorphic form of MG-water systems and MG-structured emulsions can be
59 characterized using powder X-Ray diffraction (XRD) and differential scanning calorimetry
60 (DSC). The α -gel phase has a single peak at ~ 4.2 Å in the wide angle scattering (WAXS) region
61 and a peak representing the (001) plane at ~ 55 Å in the small angle scattering region (SAXS); on
62 the other hand, the coagel phase has several diffraction peaks between 3.6 and 4.6 Å in the
63 WAXS region and a peak representing the (001) plane at 49 Å in the SAXS region.¹ The extent
64 of polymorphic transformation from the α -gel phase to the coagel phase can be described using
65 the Coagel Index (CI) determined by DSC.¹⁷ In the calculation of CI, two heating cycles are
66 applied to the MG-structured systems above T_k . The enthalpy of melting from the first heating
67 cycle (ΔH_1) represents the melting of both the α -gel and the coagel phase in aged samples while
68 the enthalpy of melting obtained from the second heating cycle (ΔH_2) represents the melting of

69 only the freshly formed α -gel phase. The CI can then be calculated by taking the ratio of $\Delta H_1/$
70 ΔH_2 .¹⁷ CI equals to 1.0 or 2.0 means that the MG-structured system is either completely in the α -
71 gel phase or the coagel phase.¹⁷ Interestingly, CI has not been previously used to characterize the
72 polymorphic transformation of MG in o/w structured emulsions. Another parameter, the sub- α -
73 Coagel Index ($CI_{\text{sub}\alpha}$), has been recently developed to determine the degree of coagel formation
74 and could possibly be used to characterize the polymorphic state of MG-structured emulsions.¹⁸
75 Similar to the determination of CI, $CI_{\text{sub}\alpha}$ is determined also from two DSC heating cycles,
76 however, the starting temperature in these cycles are set at lower than 13°C to ensure that the
77 system is in the sub- α -gel phase. The enthalpies of the phase transition from the sub- α -gel phase
78 to the α -gel phase are then obtained from the first heating cycle ($\Delta H_{\text{sub}\alpha 1}$) and the second heating
79 cycle ($\Delta H_{\text{sub}\alpha 2}$), respectively. $CI_{\text{sub}\alpha}$ is then calculated from taking the ratio of $\Delta H_{\text{sub}\alpha 1}/\Delta H_{\text{sub}\alpha 2}$.¹⁸
80 $CI_{\text{sub}\alpha}$ equals to 1.0 indicates that the system is completely in the sub- α -gel phase while $CI_{\text{sub}\alpha}$
81 equals 0.0 indicates that no sub- α -gel phase remains and the system is completely in the coagel
82 phase.

83 The stability of the α -gel phase is affected by various internal and external factors.
84 Incorporating negatively charged co-emulsifiers can increase the electrostatic repulsion between
85 MG-bilayers and slow down the polymorphic transformation from the α -gel to the coagel
86 phase.^{3,10,18} Sodium stearoyl lactylate (SSL) is a negatively charged molecule that naturally
87 crystallizes into the α form.¹ Previous studies have shown that adding 5-10 % (w/w) SSL to
88 GMS successfully improves the stability of the α -gel phase of a GMS-water hydrogel system.¹⁸
89 Other co-emulsifiers such as sodium stearate, DATEM, and phospholipids also improve the α -
90 gel stability.^{10,15,19-22} However, co-emulsifiers are greatly affected by pH and ionic strength of
91 the matrix.^{11,23,24} In terms of external factors, using slow cooling rates and avoiding shear upon

92 and after cooling were found to also enhance the stability of the α -gel phase.^{8,18,25,26}

93 Another strategy to enhance the stability of MG-structured emulsions is increasing the
94 viscosity of the water phase which improves the stability of the α -gel phase formed by MGs.
95 Xanthan gum is a commonly used stabilizer in food and cosmetic emulsions because it forms a
96 shear-thinning viscous fluid in both hot and cold water, and could increase the low-shear
97 viscosity of the water phase at low concentrations.^{27,28} Additionally, xanthan gum is surface
98 active at oil-water interfaces, which could help stabilize the emulsion by lowering the surface
99 tension and introducing electrostatic repulsion between MG-bilayers.^{28,29}

100 Previous work done by our group has investigated factors that affect the stability of MG-
101 water systems. From a more practical point of view, most food and cosmetic systems structured
102 with MGs are in the form of emulsions that contain both water and oil. This work will further
103 examine various internal and external factors that could affect the long-term stability of MG-
104 structured emulsions that contain 5 % (w/w) and 15 % (w/w) emulsifiers (*i.e.* GMS with SSL as
105 the co-emulsifier) of high water content. The internal factors examined were the concentration of
106 the co-emulsifiers and the addition of xanthan gum, while the external factors included cooling
107 rate and shear upon cooling.

108

109 **2. Experimental**

110 **2.1 Materials**

111 The structured emulsions examined contained deionized water, oil, GMS, SSL, potassium
112 sorbate and xanthan gum. The oil phase used in the emulsion was Neobee[®] M-5 oil from Stephan
113 Company supplied by Charles Tennant & Company (Canada) Limited (Weston, ON, Canada).
114 The GMS used was Alphadim 90 SBK provided by Caravan Ingredients (Lenexa, KS, USA)

115 mainly contains GMS. The SSL used was Emplex Sodium Stearoyl Lactylate provided by
116 Caravan Ingredients (Lenexa, Kansas, USA) and the xanthan gum was FASTir[®] Xanthan EC
117 (TIC GUMS, White Marsh, MD, USA). The potassium sorbate was purchased from Sigma-
118 Aldrich Canada Co. (Oakville, ON).

119

120 **2.2 Sample preparation**

121 Emulsion samples with various GMS, SSL and xanthan gum concentrations studied in
122 this work are listed in Table 1. The standard emulsions contained 5 % (w/w) emulsifier, 70%
123 (w/w) water and 25% (w/w) oil. In the water phase, 0.1 % (w/w) potassium sorbate was added in
124 all the samples while 0.07 % (w/w) xanthan gum was added to selected samples. The oil phase
125 was comprised of 25 % (w/w) oil and 5 % (w/w) emulsifiers at a 19:1 (w/w) MG: SSL or 9:1
126 (w/w) of MG: SSL ratio. Samples with higher emulsifier concentration were prepared in order to
127 improve on the signal to noise ratio of XRD signals, and these were called high-solids emulsions.
128 The high-solids emulsions contained 60 % (w/w) of water, 25% (w/w) of oil, and 15% (w/w)
129 emulsifiers.

130 Emulsions were made using the following procedure. First, both the water phase and the
131 oil phase were heated above the melting temperature of GMS (75°C) in a microwave oven. The
132 oil phase was then added into the water phase upon homogenization with a KitchenAid[®] 2 speed
133 immersion blender (Whirlpool Corporation, St. Joseph, MI, USA) until a desired consistency
134 was achieved. Emulsions for studying the effect of internal factors were quickly transferred to
135 glass bottles and cooled to room temperature on the bench while emulsions for studying the
136 effects of cooling rate and applied shear were cooled following the method used by Wang et al.¹⁸
137 Samples were prepared and analyzed in duplicate, and were stored at 45°C in capped glass jars

138 for accelerated shelf life tests.

139

140 **2.3 Melting profiles**

141 The melting profiles of the emulsions were examined with Mettler Thermal Analysis
142 DSC 1 (Mettler Toledo Canada, Mississauga, Canada). Emulsion samples around 5-10 mg were
143 weighted and hermetically sealed in aluminum pans and heated from 1 to 75°C at 10°C per
144 minute. The melting profiles of the lotion samples were analyzed using Mettler's Star^e software
145 (Mettler Toledo Canada, Mississauga, ON, Canada). The $CI_{\text{sub}\alpha}$ of MG-structured emulsions was
146 calculated as described by Wang *et al.*¹⁸

147

148 **2.4 Polymorphic forms**

149 The lamellar spacing and polymorphic forms of the emulsions with high MG
150 concentration were characterized with a Rigaku Multiflex X-ray Diffractometer (RigakuMSC
151 Inc., The Woodlands, TX, USA). This unit has a copper source ($\lambda=1.54\text{\AA}$) set at 44 kV and 40
152 mA, and the divergence slit, receiving slit, and scattering slit were set at 0.3 mm, 0.5°, and 0.5°,
153 respectively. Emulsion samples were placed onto a glass sample holder with an area of 20×20
154 mm and depth of 1 mm. Samples were examined at diffraction angles in the range $1^\circ < 2\theta < 35^\circ$
155 under the scanning rate of 1° per minute. Experiments were conducted at room temperature. The
156 XRD results were analyzed with Jade 6.0 (Material Data Inc., Livermore, CA, USA).

157

158 **2.5 Water and oil mobility**

159 The water and oil mobility in MG-structured emulsion was determined by pulsed proton
160 nuclear magnetic resonance (NMR) using a Bruker mq20 Series NMR Analyzer (Bruker, Milton,

161 ON, Canada). The ^1H -NMR unit was connected to a circulating water bath set at $17^\circ\text{C}\pm 0.5^\circ\text{C}$ to
162 achieve $20^\circ\text{C}\pm 0.5^\circ\text{C}$ in the measurement cell. Samples were prepared and the time constant from
163 T_2 relaxation was determined following methods published by Rogers et al.³⁰ and Goldstein *et*
164 *al.*²⁵

165 An inverse Laplace transform was applied to the free induction decays using CONTIN
166 application along with Minispec software version 2.3 (Bruker, Milton, ON, Canada). The relative
167 distribution of the number of protons relaxing at a given moment with their respective rate
168 constants was computed with the CONTIN application. The median values of the relaxation
169 times in each population were determined using PeakFit v4.12 (Systat Software Inc, San Jose,
170 CA, USA) assuming a Gaussian distribution.

171

172 3. Results and Discussion

173 3.1 $\text{CI}_{\text{sub}\alpha}$ in MG-structured emulsions

174 Figure 1 shows the melting and crystallization profiles of freshly prepared standard
175 emulsion structured with 1:19 (w/w) SSL: GMS. The two exothermic peaks (*i.e.*, 1st and 2nd
176 heating cycle) and the endothermic peak (*i.e.*, cooling) at $\sim 15^\circ\text{C}$, representing the phase
177 transition between the sub- α -gel phase and the α -gel phase, displayed similar shape and area
178 under the peak. On the other hand, the exothermic and endothermic peaks at $\sim 60^\circ\text{C}$, representing
179 the melting or crystallization of the α -gel phase, displayed different shapes and areas between the
180 first heating cycle, the second heating cycle, and the crystallization cycle. The enthalpies of
181 melting and crystallization of the sub- α -gel phase in the first heating, crystallization, and the
182 second heating cycles were 1.24, 1.40, and 1.25 J/g, while that of the α -gel gel phase were 4.55,
183 4.03, and 3.25 J/g. When freshly prepared, the sub- α -gel phase and the α -gel phase should have

184 the sample enthalpy of melting in the first and the second heating cycles because no coagel phase
185 is formed. However, results only showed the same enthalpy of melting for the sub- α -gel phase
186 but not for the α -gel phase. The difference in shape and area between the melting peaks of the α -
187 gel phase obtained from the two heating cycles suggests that changes induced by heating may be
188 affecting emulsion structure beyond a mere reversible change in polymorphic state. Furthermore,
189 differences between the and second heating cycle thermograms suggest that these changes are
190 irreversible. As a result, changes in CI are due to both changes in emulsion structure as well as
191 polymorphic form, while changes in $CI_{\text{sub}\alpha}$ are strictly due to change in polymorphic form.
192 Looking at the indicators used for the polymorphic transformation from the α -gel phase to the
193 coagel phase in MG-structured emulsions, CI takes into account both the changes in emulsion
194 structure and polymorphic form while $CI_{\text{sub}\alpha}$ alpha only takes that of the polymorphic form.
195 Therefore $CI_{\text{sub}\alpha}$ is a better indicator of the degree of the polymorphic transformation of MG-
196 structured emulsions.

197

198 3.2 Internal factors

199 Figure 2 (a-c) presents the melting profiles of high-solids emulsions when they were
200 freshly made and after storage at 45°C for four weeks. All samples showed two exothermic
201 peaks at ~15°C and at 55-60°C when freshly made, representing the phase transition from the
202 sub- α -gel phase to the α -gel phase and the melting of the α -gel phase respectively. After storing
203 the 1:19 (w/w) SSL: GMS emulsion for four weeks, the second melting peak was very broad,
204 ranging from 52 to 65°C, including three overlapping peaks (Figure 2a). The observation of these
205 overlapping peaks suggests possible phase separation or destabilization of the emulsion. On the
206 other hand, the emulsion with higher SSL in GMS ratios (*i.e.*, 1:9 (w/w) SSL: GMS) displayed

207 only two melting peaks – a broad melting peak at $\sim 58^{\circ}\text{C}$ with an overlapping peak appearing at
208 60°C after storage at 45°C for four weeks (Figure 2b). The melting profile of emulsions
209 containing 1:19 (w/w) SSL: GMS with xanthan gum also showed a very broad melting peak
210 including multiple peaks after four weeks of storage at 45°C . Comparing the three emulsion
211 formulations, one can notice that the one with higher SSL content (1:9 (w/w) SSL: GMS)
212 showed similar melting curves after four weeks of incubation than when freshly prepared,
213 indicating that it was structurally more stable.

214 The $CI_{\text{sub}\alpha}$ for both high-solids emulsions (Figure 2d) and standard emulsions (Figure 2e)
215 decreased and approached zero upon aging; however, $CI_{\text{sub}\alpha}$ decreased slower in high-solids
216 emulsions. Such decrease in $CI_{\text{sub}\alpha}$ indicates that the polymorphic transformation from the sub- α -
217 gel phase or the α -gel phase to the coagel phase in all the systems, and the polymorphic
218 transformation were slowed down slightly by higher emulsifier (GMS and SSL) concentrations.
219 Similar trends in the change of $CI_{\text{sub}\alpha}$ suggest both the high-solids and standard samples
220 transformed from the α -gel phase to the coagel phase. Therefore, to be able to obtain a higher
221 signal to noise ratio, high-solids emulsions were examined with powder XRD.

222 The XRD patterns of fresh high-solids' emulsions and after storage at 45°C for four
223 weeks are summarized in Figure 3. The three formulations displayed similar SAXS peaks at
224 55\AA , 25\AA and 16\AA and WAXS peaks at 4.17\AA when freshly prepared (Figure 3a and 3b),
225 indicating they were all in the α -gel phase. After incubation at 45°C for four weeks, samples with
226 higher SSL content and with xanthan gum were in the α -gel phase (WAXS peak at 4.17\AA), while
227 samples with 1:19 (w/w) SSL: GMS transformed into the coagel phase (WAXS peaks between
228 3.6 and 4.6\AA) (Figure 3d). Two peaks at 55\AA and 49\AA were observed from 1:9 SSL: GMS and
229 1:19 with xanthan emulsions (Figure 3c), suggesting the co-existence of lamellar structures with

230 two different thicknesses, specifically the α -gel phase and the emerging coagel phase upon aging.
231 The broad peaks in the SAXS region, diffracted by these two emulsions, suggest that the GMS
232 bilayers remained hydrated and less crystalline. Emulsions structured with 1:19 (w/w) SSL:
233 GMS, on the other hand, displayed well-defined SAXS peaks at 49Å, 24.5Å, 16.5Å, 12.4Å and
234 8.3Å (Figure 3c), suggesting the presence of the more crystalline and less swollen lamellar
235 structures compared with freshly prepared systems.³¹ In summary, results show that increasing
236 SSL concentration and adding xanthan gum increases the water swelling capacity of lamellar
237 structures formed by GMS, which in turn improves the stability of the α -gel phase of the
238 structured emulsions.

239 The distributions of pulse NMR T2 relaxation times are summarized in Figure 4. The
240 time constants of the primary components of MG-structured emulsions, water and oil, were
241 determined. The measured T2 time constant for water was 2479 ms, in agreement with the
242 literature reported value,²⁵ and that for Neobee[®] oil were 48, 104, and 215 ms. No time constant
243 that is correlated with the presence of free water was observed in any of the MG-structured
244 emulsions, indicating that water in all the emulsions was bound within the multi-lamellar
245 structure and thus displayed restricted mobility. The relaxation distribution of the standard
246 emulsion structured with 1:19 (w/w) SSL: GMS shifted to higher time constant after one week
247 and four weeks (Figure 4a), indicating increased mobility and decreased water and oil binding.
248 The sample structured with 1:9 (w/w) SSL: GMS displayed a narrower distribution of T2
249 relaxation times, but were also shifted to longer times upon aging (Figure 4b). Higher T2
250 relaxation time was observed from samples structured with 1:19 (w/w) SSL: GMS with xanthan
251 gum at day 0 (Figure 4c), this indicates that the addition of xanthan gum initially leads to higher
252 water and oil mobility than the other two formulations. However, throughout storage for four

253 weeks, only small shifts in the distribution of relaxation times were observed, indicating that
254 xanthan gum helps increase the stability of the structured emulsion. The relaxation distributions
255 of high-solids emulsions are not presented because their distribution of the three populations was
256 similar with those of the standard emulsions.

257 The computed median values of the time constants of standard and high-solids emulsions
258 are presented in Figure 5. The relaxation distribution of the standard emulsions that contain 1:9
259 (w/w) SSL: GMS and with xanthan gum showed less of a T2 increase in time for population 3
260 compared with the emulsion structured with less GMS without xanthan (*i.e.* 1:19 (w/w) SSL:
261 GMS) (Figure 5 a-c). This therefore shows that the presence of xanthan gum or higher SSL
262 content in the structured emulsions results in lower water and oil had mobility and strong
263 binding. Compared to standard emulsions, high-solids systems (Figure 5 d-f) displayed lower
264 time constants because these systems contain less liquid, but they showed a similar increasing
265 trend upon aging.

266 Higher solids content increased the overall water and oil-binding capacity of the lamellar
267 structure formed by GMS and decreased T2 relaxation times, however the water and oil mobility
268 in these systems also increased upon aging. This increase in water and oil mobility in GMS-
269 structured emulsions is caused by micro scale release of water due to the polymorphic
270 transformation from the α -gel phase to the coagel phase.

271 Results suggest that internal factors which improve the stability of the α -gel phase in
272 MG-structured emulsion are similar to those that improve the stability of the α -gel phase of MG-
273 water systems.¹⁸ Increasing the concentration of α -tending co-emulsifiers (SSL) and adding
274 xanthan gum increased the α -gel stability of MG-structured emulsions by increasing water layer

275 thickness in the lamellar structure and enhancing water and oil binding capacity in the structured
276 emulsions.

277

278 3.3 External factors

279 Fast cooling rate, slow cooling rate, and cooling with shear were examined as external
280 factors that potentially affect the stability of MG-structured emulsions. As previously discussed,
281 the standard and high-solids samples displayed similar trends in changes that occur in their
282 structural and polymorphic properties, only $CI_{\text{sub}\alpha}$ for high-solids samples are presented in Figure
283 6. All the formulations displayed a large decrease in $CI_{\text{sub}\alpha}$ from 1.0 to 0.0 within two weeks
284 when cooled under shear during preparation, indicating that shear leads to faster polymorphic
285 transition from the α -gel phase to the coagel phase in MG-structured emulsions. Emulsions
286 structured with 1:19 (w/w) SSL: GMS, with and without added xanthan gum (Figure 6a and 6c),
287 both maintained a $CI_{\text{sub}\alpha}$ of ~ 1.0 for longer than six weeks when cooled at a slow cooling rate
288 during preparation, while their $CI_{\text{sub}\alpha}$ decreased to 0.0 in three weeks when cooled at a fast rate
289 during preparation. Slow cooling therefore allowed the formation of more stable sub- α -gel phase
290 and α -gel phase in these MG-structured emulsions. The emulsion structured with 1:9 (w/w) SSL:
291 GMS (Figure 6b) showed a similar decrease in $CI_{\text{sub}\alpha}$ under fast and slow cooling rates but $CI_{\text{sub}\alpha}$
292 decreased slowly to 0.0 under a fast cooling rate after six weeks.

293 WAXS patterns of high-solids emulsions prepared using a slow cooling rate, a fast
294 cooling rate, in the presence and absence of shear are compared in Figure 7. All emulsions were
295 in the α -gel phase when freshly prepared, characterized by a single WAXS spacing at 4.17Å.
296 Emulsions structured with 1:19 (w/w) SSL: GMS with and without xanthan gum under slow
297 cooling rate preserved the α -gel phase for up to six weeks, characterized by single WAXS peak

298 at 4.17Å in Figure 7a. The emulsion structured with 1:9 (w/w) SSL: GMS diffracted a major
299 WAXS peak at 4.17Å with minor peaks between 3.6 and 4.6Å after six weeks, suggesting that
300 the system had started to transform into the coagel phase. Under fast cooling rate (Figure 7b),
301 only the emulsion structured with 1:9 (w/w) SSL: GMS displayed a WAXS peak representing
302 the α -gel phase at 4.17Å, while the other two samples were already in the coagel phase, indicated
303 by peaks between 3.6 and 4.6Å. After one week of storage, all samples cooled under shear
304 displayed peaks between 3.6 and 4.6Å (Figure 7c), and only emulsions structured with higher
305 SSL content (*i.e.* 1:9 (w/w) SSL: GMS) still displayed a small peak at 4.17Å. Applied shear upon
306 cooling therefore accelerated the formation of the coagel phase, in agreement with results
307 obtained from DSC experiments.

308 The T2 relaxation times of MG-structured emulsions prepared under various cooling
309 conditions and incubated at 45°C are presented in Figure 8. No further time points were
310 measured after the $CI_{\text{sub}\alpha}$ decreased to 0.0 (*i.e.*, when the system was completely transformed into
311 the coagel phase). For all the formulations, samples prepared under slow cooling rates showed
312 smaller T2 relaxation times compared to those prepared under high cooling rates and under
313 shear. This therefore indicates that the water and oil had less mobility and were highly bound
314 within the multi-lamellar structured when prepared under slow cooling rates compared with
315 prepared using fast cooling rates or shear. The emulsion structured with 1:19 (w/w) SSL: GMS
316 with xanthan gum showed the smallest increase in T2 relaxation times after 60 days among the
317 three formulations (Figure 8g), and was therefore considered the most stable. On the other hand,
318 the emulsion structured with 1:9 (w/w) SSL: GMS had a smaller T2 relaxation time when
319 prepared using a fast cooling rate (Figure 8e) or under shear relative to the other two

320 formulations (Figure 8f). This suggests that higher SSL levels improved the emulsion's stability
321 towards higher cooling rate and shear.

322 Results suggested that slow cooling rates promoted the formation of a more stable α -gel
323 phase while fast cooling rate and applied shear accelerated the polymorphic transformation from
324 the α -gel phase to the coagel phase in GMS-structured emulsions. This is in agreement with
325 previous studies on GMS-water hydrogels and MG-structured emulsions.^{8,18,25,26} Even though
326 previous work showed that slow cooling rates promote the formation of larger droplets⁸, higher
327 α -gel stability was still achieved in emulsions with 1:19 (w/w) SSL:GMS with or without
328 xanthan gum under slow cooling rates. One possible explanation to such phenomenon is that
329 slow cooling rates provide MG molecules with more time to mix with co-emulsifiers, oil, and
330 water to self-assemble into fully hydrated lamellar structures.³² On the other hand, fast cooling
331 rates and the application of shear upon cooling promote the nucleation into the coagel phase and
332 disrupt the formation of continuous lamellar hydrate, resulting in the enhancement of water
333 release from the multi-lamellar structure.¹⁸ Additionally, the behaviour of the emulsion systems
334 under different cooling conditions was affected by composition as it was found that higher SSL
335 content possibly increased the emulsions' stability against higher cooling rates and shear.

336

337 **4. Conclusion**

338 This work examined internal and external factors that affect the polymorphic
339 transformation and stability of GMS-structured o/w emulsions. The sub- α Coagel Index was used
340 for the first time as an effective parameter to characterize the degree of coagel formation in MG-
341 structured emulsions.

342 The internal and external factors examined in this work were shown to affect the
343 polymorphic form and stability of GMS-structured emulsions in complex ways. Increasing the
344 concentration of α -tending co-emulsifiers, specifically SSL, improved the stability of GMS-
345 structured emulsions. The addition of xanthan gum also improved emulsion stability and the
346 mechanism possibly involved enhancing electrostatic repulsion between GMS lamellae and
347 increasing the viscosity of the water phase. Higher emulsion stability was also obtained when the
348 emulsion was formed using a slow cooling rate, while cooling under shear was found to decrease
349 emulsion stability. Increasing SSL concentration improved emulsion stability against faster
350 cooling rates and shear.

351 The effects of internal and external factors on the stability of the α -gel phase in MG-
352 structured o/w emulsions were similar to their effects on MG-water systems. Understanding the
353 nature and dynamics of simple MG-water systems thus successfully predicted the behaviour in
354 more complex MG-structured emulsion systems with high water content.

355

356 5. Acknowledgements

357 This work was funded by Natural Sciences and Engineering Research Council of Canada.
358 The authors would like to thank Ms. Karissa Salama-Frakes for her help with NMR data
359 processing.

360

361 6. References

- 362 1. N. J. Krog, in *Food Emulsions*, eds. S. E. Friberg and K. Larsson, Marcel Dekker, New
363 York, 3rd edn., 1997.
- 364 2. A. G. Marangoni and S. H. J. Idziak, 2010. *US Pat.* 7,718,210 B2.

- 365 3. A. G. Marangoni, S. H. J. Idziak, C. Vega, H. Batte, M. Ollivon, P. S. Jantzi, and J. W. E.
366 Rush, *Soft Matter*, 2007, **3**, 183.
- 367 4. H. D. Batte, A. J. Wright, J. W. Rush, S. H. J. Idziak, and A. G. Marangoni, *Food*
368 *Biophys.*, 2007, **2**, 29–37.
- 369 5. A. Goldstein and K. Seetharaman, *Food Res. Int.*, 2011, **44**, 1476–1481.
- 370 6. S. Calligaris, L. Manzocco, F. Valoppi, and M. C. Nicoli, *Food Res. Int.*, 2013, **51**, 596–
371 602.
- 372 7. A. I. Blake and A. G. Marangoni, *Food Res. Int.*, 2015, **74**, 284–293.
- 373 8. H. D. Batte, A. J. Wright, J. W. Rush, S. H. J. Idziak, and A. G. Marangoni, *Food Res.*
374 *Int.*, 2007, **40**, 982–988.
- 375 9. N. K. Ojijo, I. Neeman, S. Eger, and E. Shimoni, *J. Sci. Food Agric.*, 2004, **84**, 1585–
376 1593.
- 377 10. I. Heertje, E. . Roijers, and H. A. C. . Hendrickx, *LWT - Food Sci. Technol.*, 1998, **31**,
378 387–396.
- 379 11. N. Krog and K. Larsson, *Chem. Phys. Lipids*, 1968, **2**, 129–143.
- 380 12. K. Larsson and N. Krog, *Chem. Phys. Lipids*, 1973, **10**, 177–180.
- 381 13. N. Krog and A. P. Borup, *J. Sci. Fd Argic*, 1973, **24**, 691–701.
- 382 14. K. Larsson, K. Fontell, and N. Krog, *Chem. Phys. Lipids*, 1980, **27**, 321–328.
- 383 15. A. Zetzl, M. Ollivon, and A. Marangoni, *Cryst. Growth Des.*, 2009, **9**, 3928–3933.
- 384 16. F. C. Wang and A. Marangoni, *RSC Adv.*, 2014, **4**, 50417–50425.
- 385 17. G. Cassin, C. de Costa, J. P. M. van Duynhoven, and W. G. M. Agterof, *Langmuir*, 1998,
386 **14**, 5757–5763.
- 387 18. F. C. Wang and A. Marangoni, *RSC Adv.*, 2015, **5**, 43121–43129.
- 388 19. M. B. Munk, A. G. Marangoni, H. K. Ludvigsen, V. Norn, J. C. Knudsen, J. Risbo, R.
389 Ipsen, and M. L. Andersen, *Food Res. Int.*, 2013, **54**, 1738–1745.
- 390 20. A. Sein, J. a Verheij, and W. G. M. Agterof, *J. Colloid Interface Sci.*, 2002, **249**, 412–422.
- 391 21. J. P. M. van Duynhoven, I. Broekmann, A. Sein, G. M. P. van Kempen, G.-J. W.
392 Goudappel, and W. S. Veeman, *J. Colloid Interface Sci.*, 2005, **285**, 703–10.

- 393 22. L. Rydhag and I. Wilton, *J. Am. Oil Chem. Soc.*, 1981, **58**, 830–837.
- 394 23. L. Mao, S. Calligaris, L. Barba, and S. Miao, *Frin*, 2014, **58**, 81–88.
- 395 24. F. C. Wang and A. G. Marangoni, *RSC Adv.*, 2015, **submitted**.
- 396 25. A. Goldstein, A. Marangoni, and K. Seetharaman, *Food Biophys.*, 2012, **7**, 227–235.
- 397 26. S. Da Pieve, S. Calligaris, E. Co, M. C. Nicoli, and A. G. Marangoni, *Food Biophys.*,
398 2010, **5**, 211–217.
- 399 27. E. Dickinson, *J. Sci. Food Agric.*, 2013, **93**, 710–21.
- 400 28. M. Izydorzcyk, S. W. Cui, and Q. Wang, in *Food Carbohydrates - Chemistry, Physical*
401 *Properties, and Applications*, CRC Press, Boca Raton, Florida, 2005.
- 402 29. M. Hennock, R. R. Rahalkar, and P. Richmond, *J. Food Sci.*, 1984, **49**, 1271–1274.
- 403 30. M. A. Rogers, A. J. Wright, and A. G. Marangoni, *Soft Matter*, 2008, **4**, 1483–1490.
- 404 31. F. Peyronel and R. Campos, in *Structure-Function Analysis of Edible Fats*, ed. A. G.
405 Marangoni, AOCS Press, Urbana, 2012, pp. 235–294.
- 406 32. J. F. Toro-vazquez, E. Dibildox-alvarado, and V. Herrera-coronado, in *Crystallization and*
407 *Solidification Properties of lipids*, eds. N. Widlak, R. Hartel, and S. Narie, AOCS Press,
408 Champaign, Illinois, 2001, pp. 53–78.

409

410

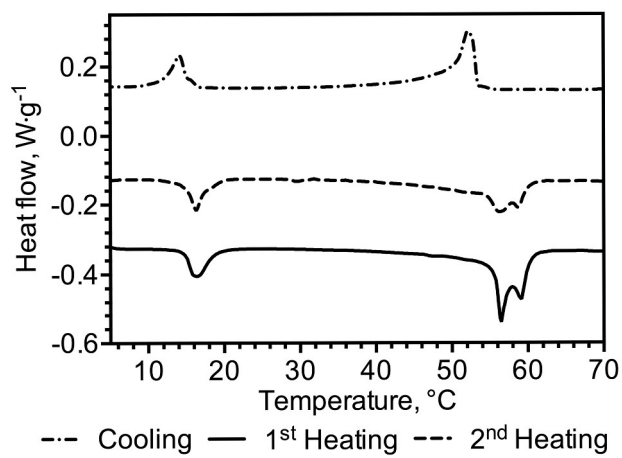
411 **Tables**

412 Table 1. Formulation of MG-structured emulsions. Ingredients are listed in % (w/w).

		Water phase			Oil phase		
		Water	Potassium sorbate	Xanthan gum	Oil	GMS	SSL
Standard emulsion	1:19 SSL: GMS	69.9	0.1	0	25	4.75	0.25
	1:19 SSL: GMS with xanthan gum	69.83	0.1	0.07	25	4.75	0.25
	1:9 SSL: GMS	69.9	0.1	0	25	4.5	0.5
High MG emulsion	1:19 SSL: GMS	59.9	0.1	0	25	14.25	0.75
	1:19 SSL: GMS with xanthan gum	59.84	0.1	0.06	25	14.25	0.75
	1:9 SSL: GMS	59.9	0.1	0	25	13.5	1.5

413

414

415 **Figures**

416

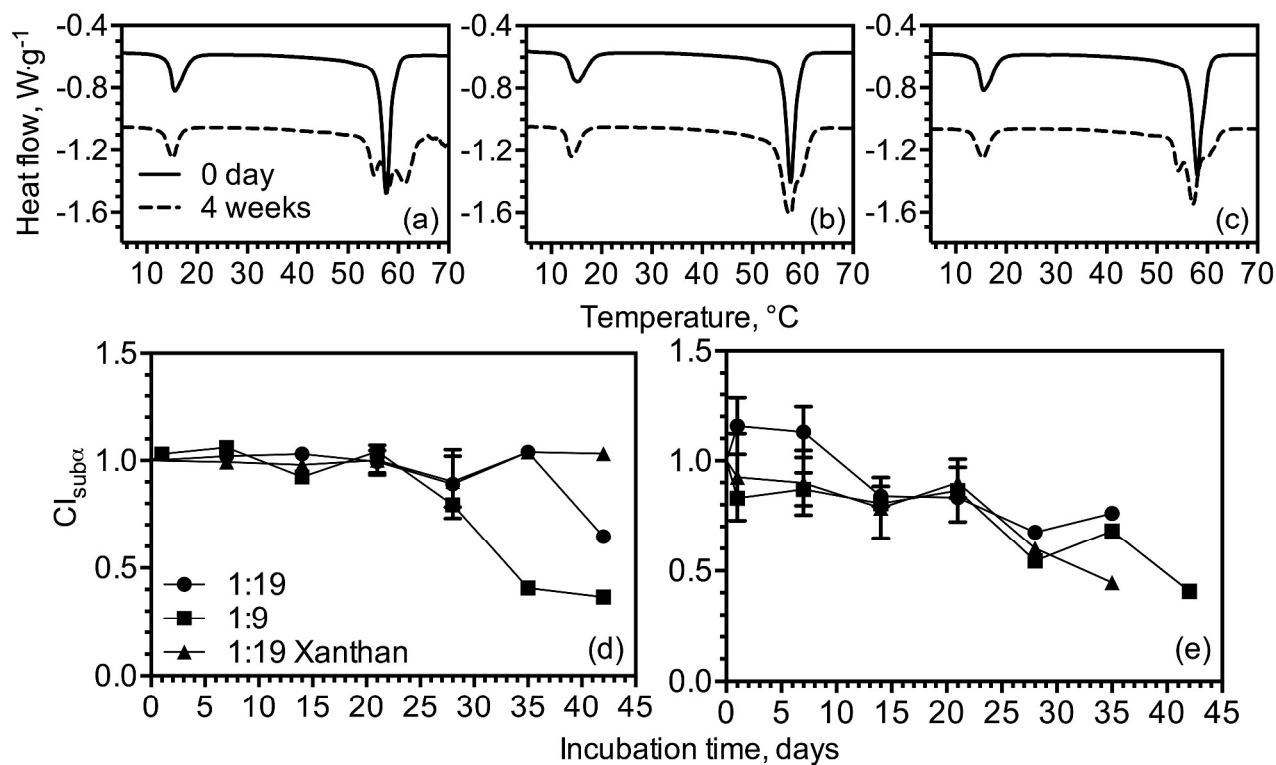
417 Figure 1. DSC Melting and crystallization curves of freshly prepared standard emulsion

418 structured with 1:19 (w/w) SSL: GMS.

419

420

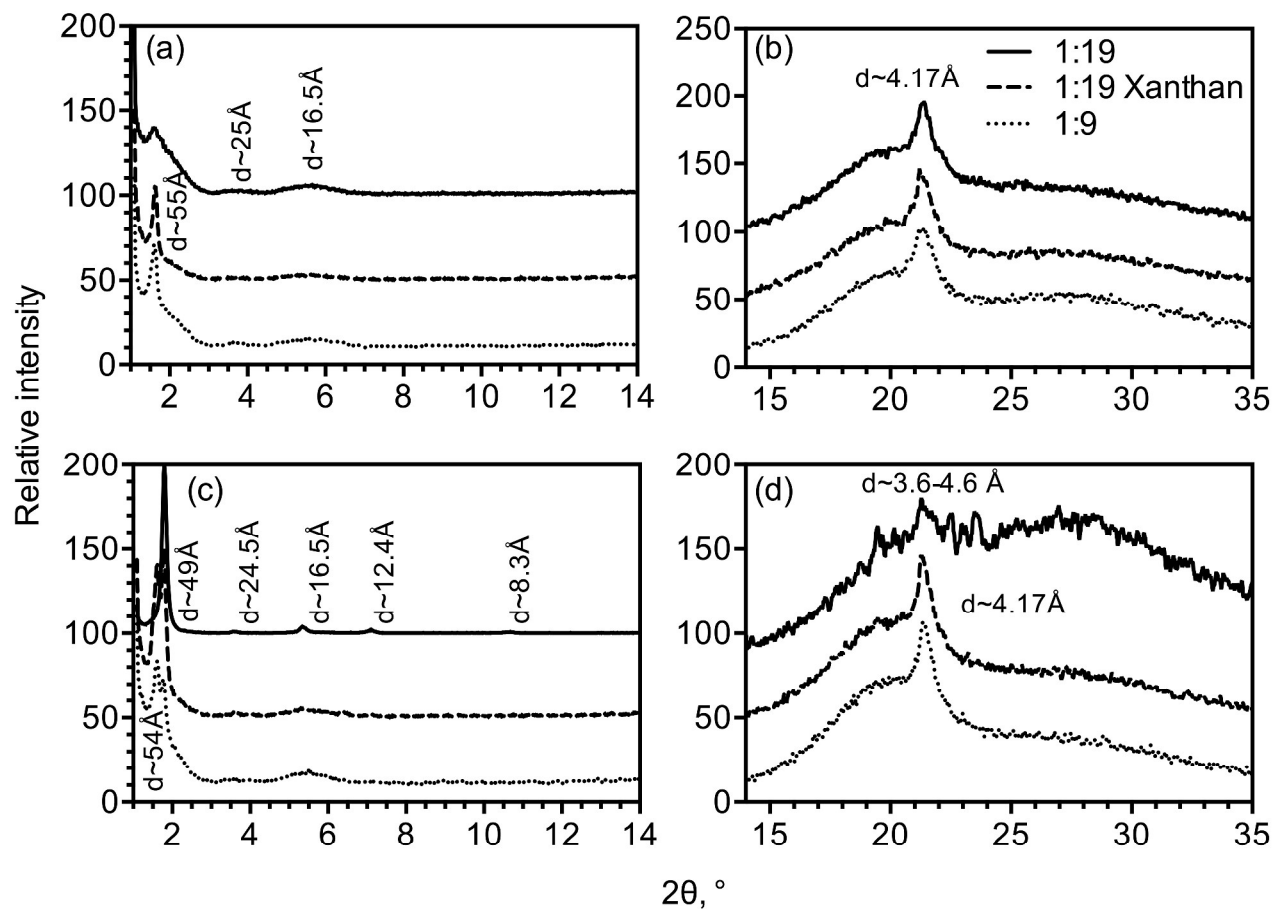
421



422

423 Figure 2. DSC melting curves of high-solid emulsions that contain (a) 1:19 (w/w) SSL: GMS, (b)
 424 1:9 (w/w) SSL: GMS, and (c) 1:19 (w/w) SSL: GMS with Xanthan gum when freshly prepared
 425 and after four weeks of incubation at 45°C, and the calculated $CI_{sub\alpha}$ of (d) high-solid and (e)
 426 standard emulsions.

427



428

429 Figure 3. XRD patterns of high-solid emulsions. (a) SAXS and (b) WAXS of freshly prepared

430 samples, and (c) SAXS and (d) WAXS of samples stored at 45°C for four weeks.

431

432

433

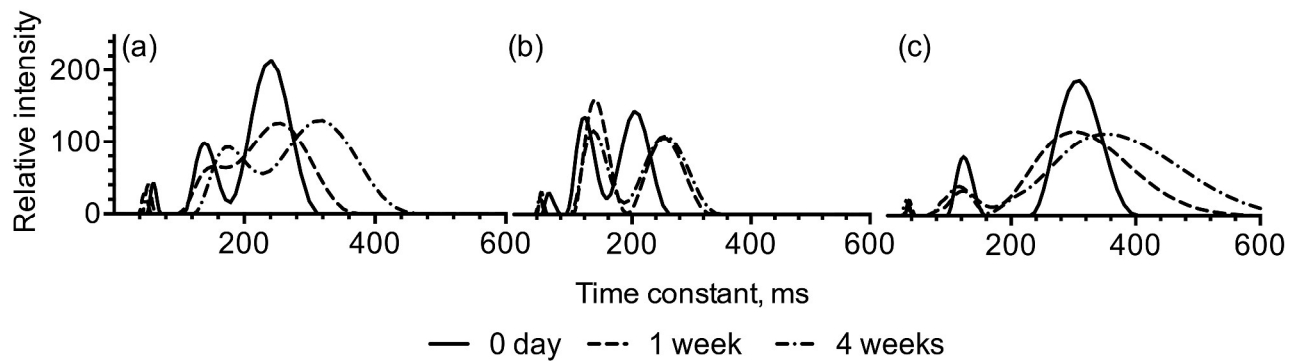
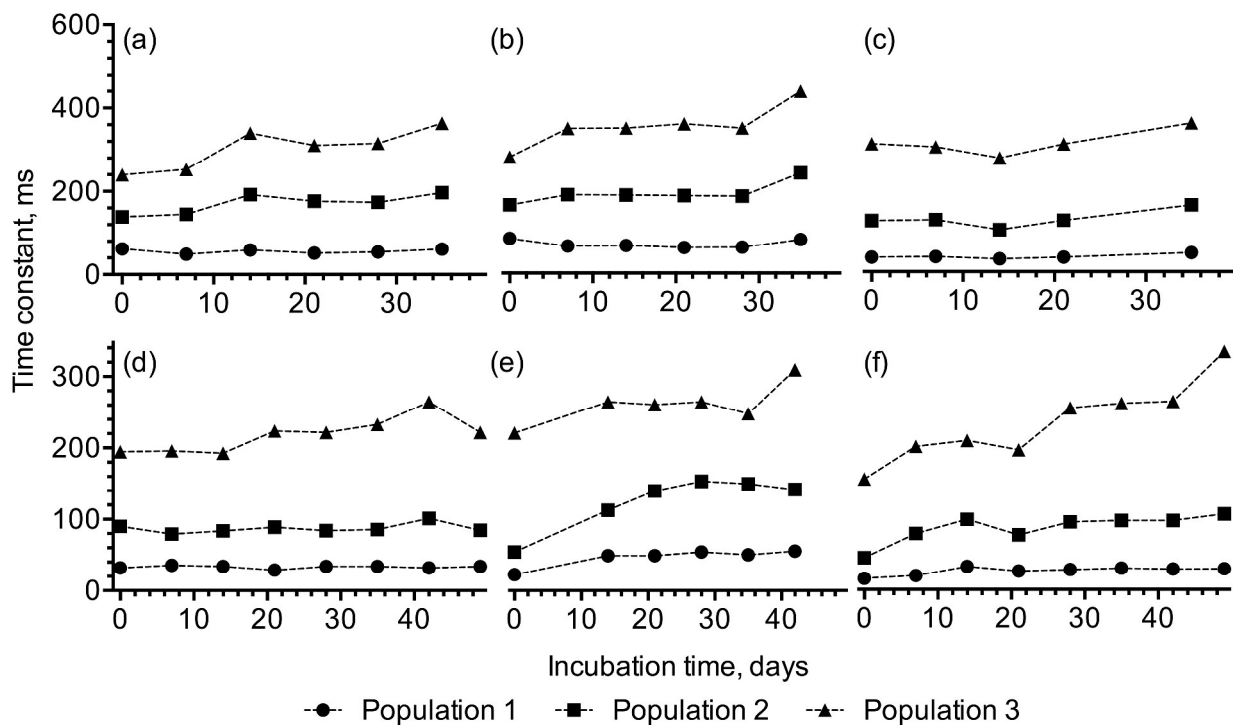
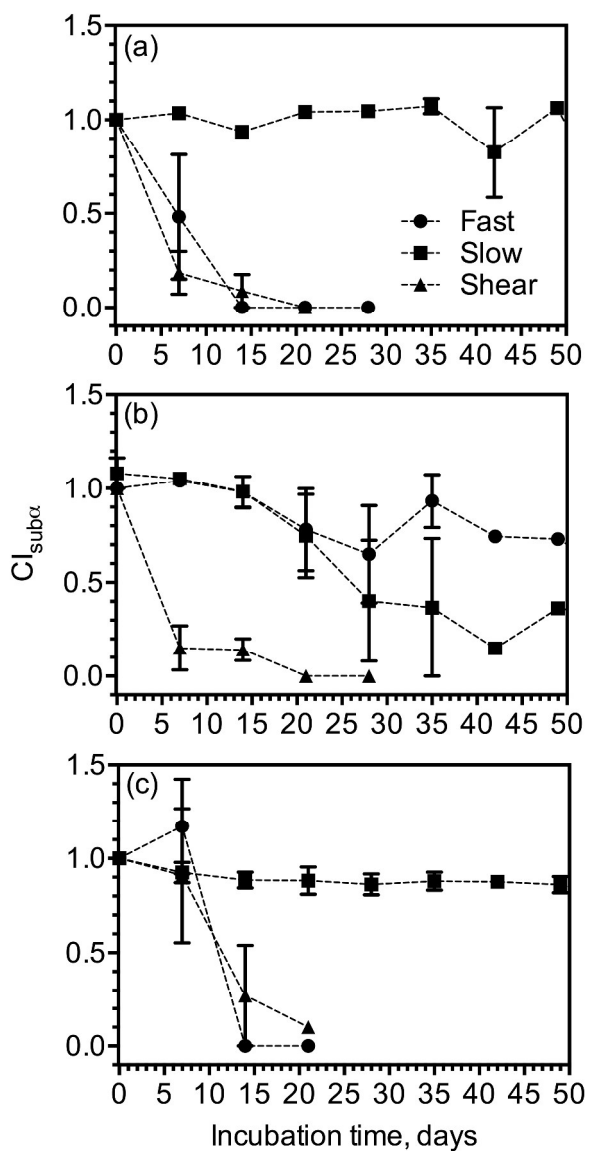


Figure 4. T2 relaxation distribution of standard emulsions structured with (a) 1:19 (w/w) SSL:GMS, (b) 1:9 (w/w) SSL:GMS, and (c) 1:19 (w/w) SSL:GMS with xanthan gum.



442

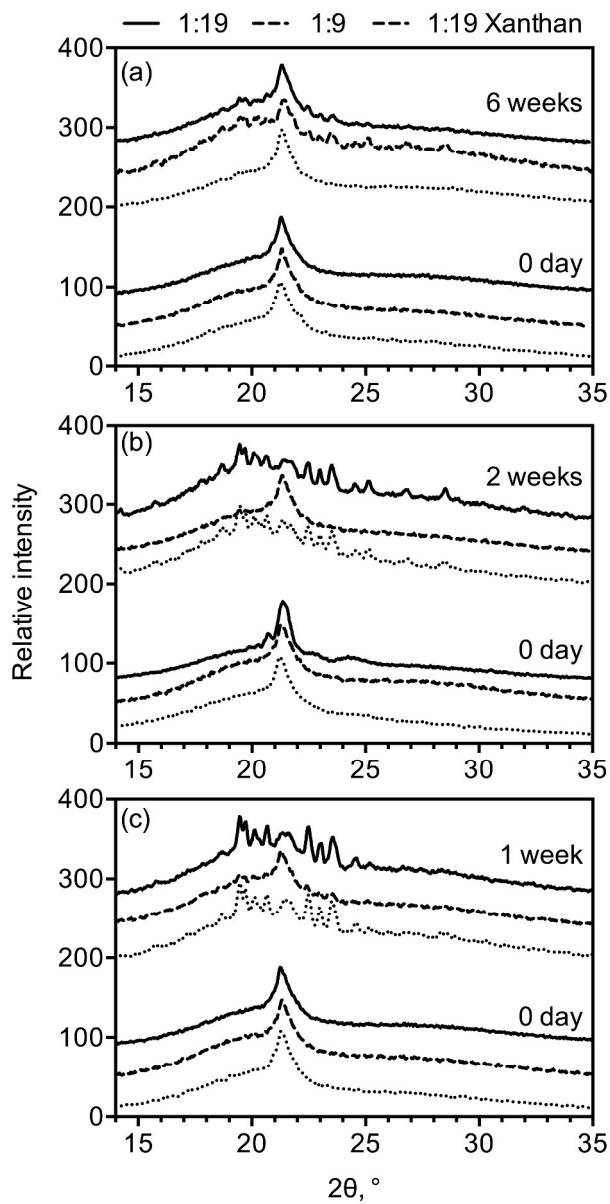
443 Figure 5. Median values of T2 time constants of standard emulsions structured with (a) 1:19
 444 (w/w) SSL: GMS, (b) 1: 9 (w/w) SSL: GMS, and (c) 1:19 (w/w) SSL: GMS with xanthan gum,
 445 and that of high-solid emulsions structured with (d) 1:19 (w/w) SSL: GMS, (e) 1: 9 (w/w) SSL:
 446 GMS, and (f) 1:19 (w/w) SSL: GMS with xanthan gum.



447

448 Figure 6. Calculated $CI_{sub\alpha}$ of high-solid emulsions structured with (a) 1:19 (w/w) SSL: GMS,
 449 (b) 1: 9 (w/w) SSL: GMS, and (c) 1:19 (w/w) SSL: GMS with xanthan gum under slow cooling
 450 rate, fast cooling rate, and cooling with shear.

451

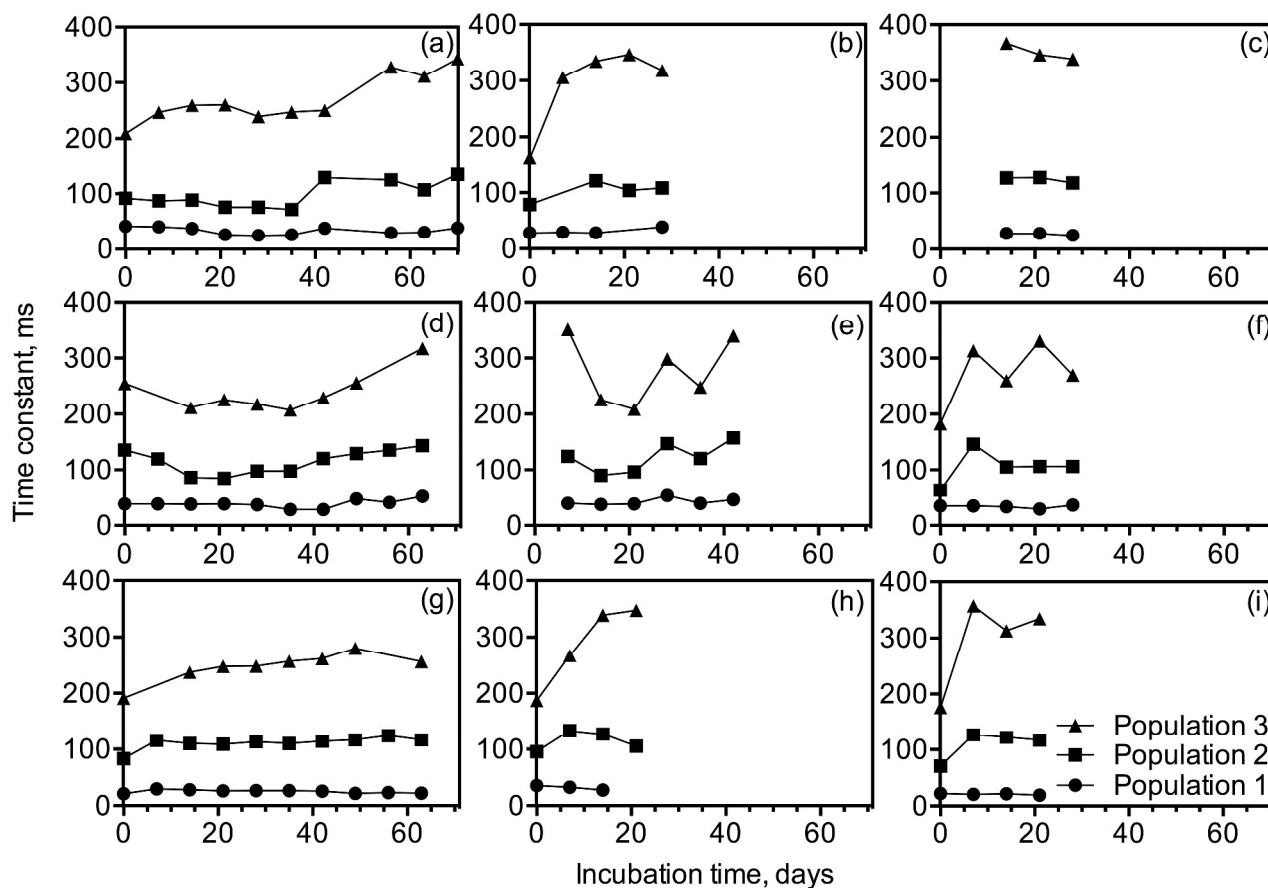


452

453 Figure 7. WAXS patterns of high-solid emulsions processed (a) under slow and (b) fast cooling

454 rates, and (c) cooled with shear.

455



456

457 Figure 8. Change in the three populations of time constant obtained from T2 relaxation of high-

458 solid emulsions structured with 1:19 (w/w) SSL: GMS (a) under slow cooling, (b) under fast

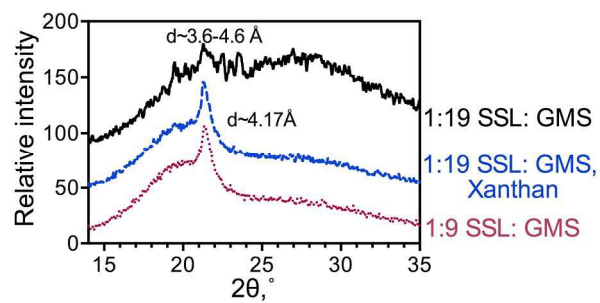
459 cooling, and (c) cooling with shear; 1:9 (w/w) SSL: GMS (d) under slow cooling, (e) under fast

460 cooling, and (f) cooling with shear; 1:19 (w/w) SSL: GMS with xanthan gum (g) under slow

461 cooling, (h) under fast cooling, and (i) cooling with shear.

462

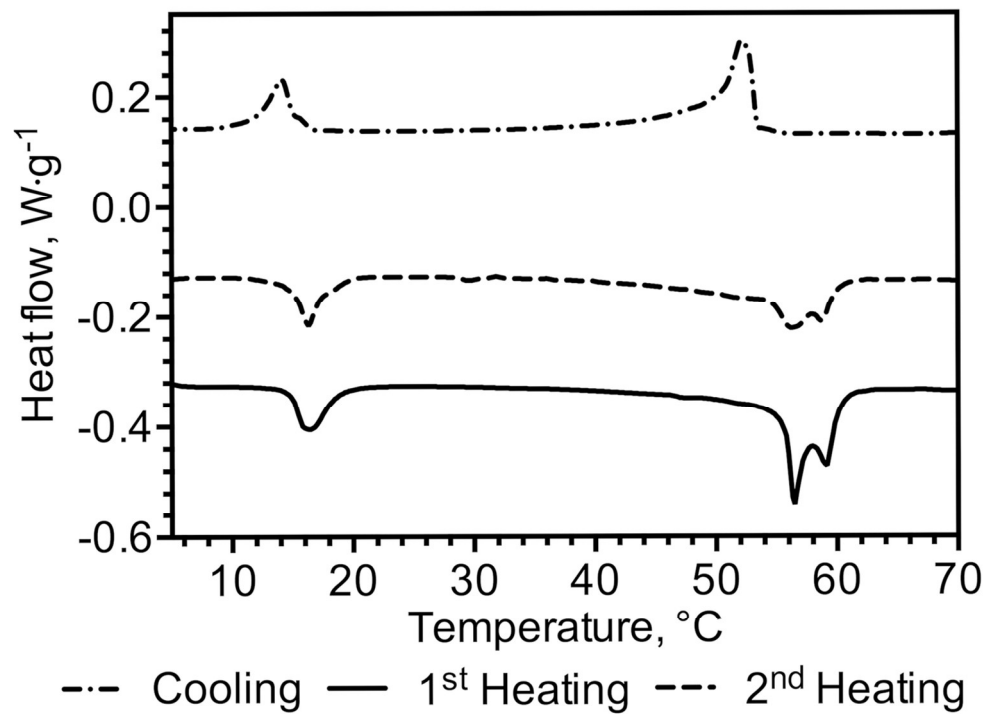
463 **For TOC Use Only**



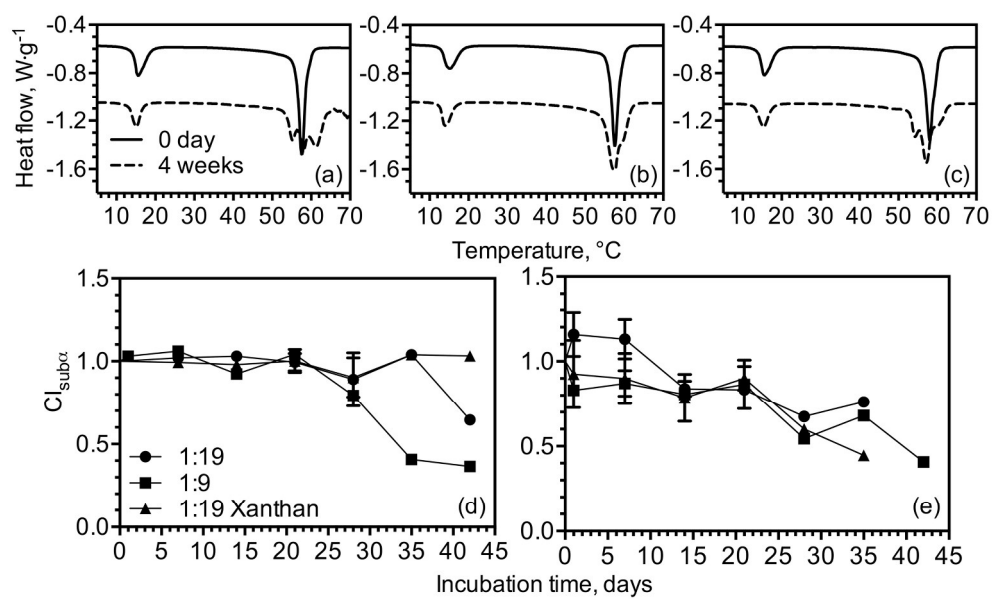
464

465 High SSL concentration, xanthan gum, and slow cooling rates without shear could stabilize the

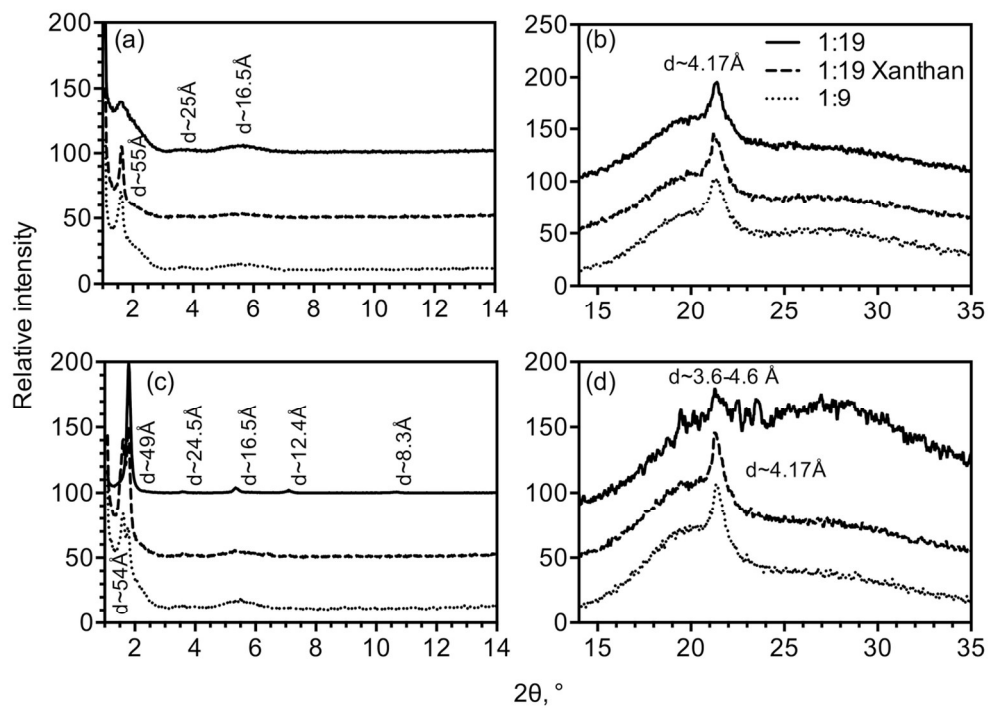
466 α -gel phase of MG-structured emulsion.



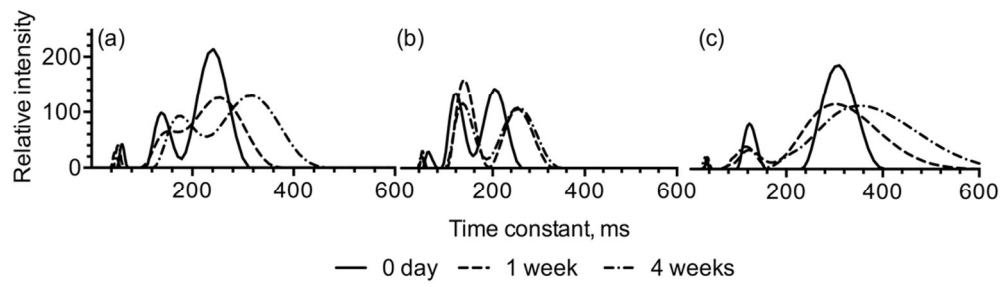
61x44mm (600 x 600 DPI)



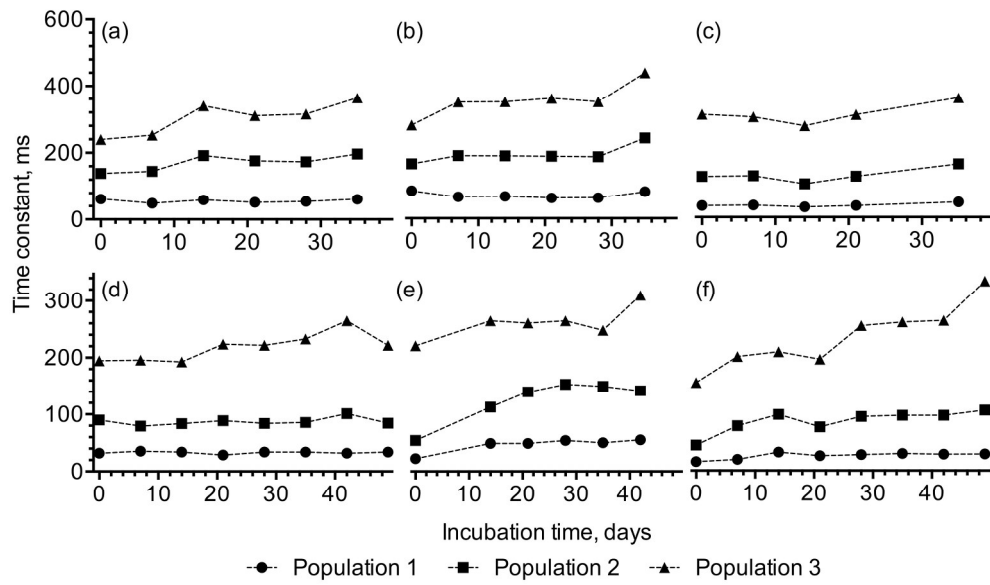
103x63mm (600 x 600 DPI)



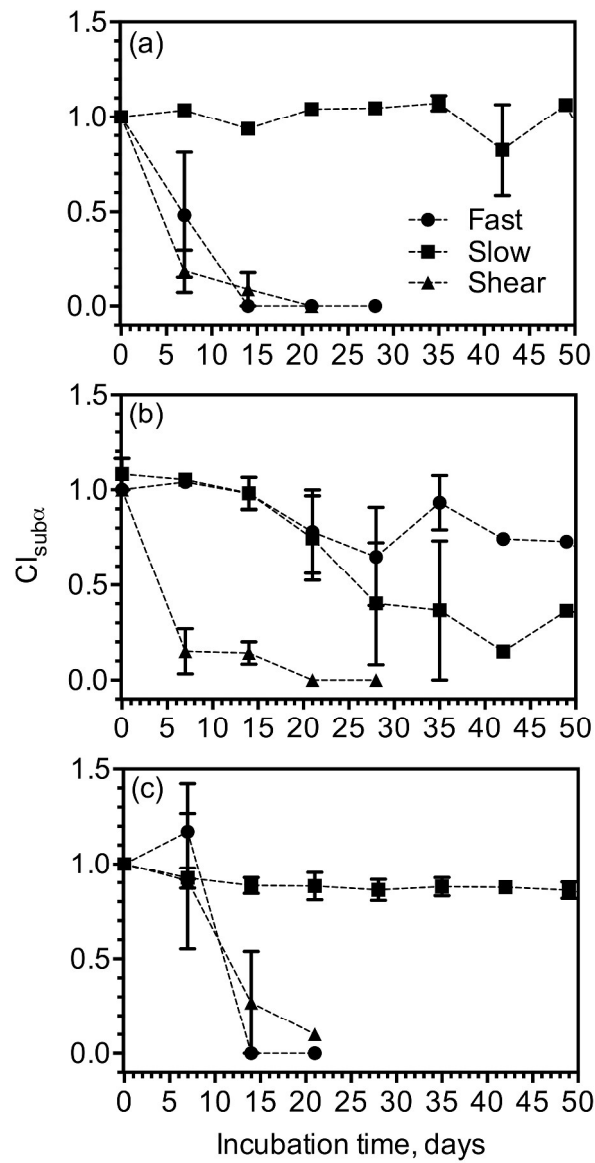
123x87mm (300 x 300 DPI)



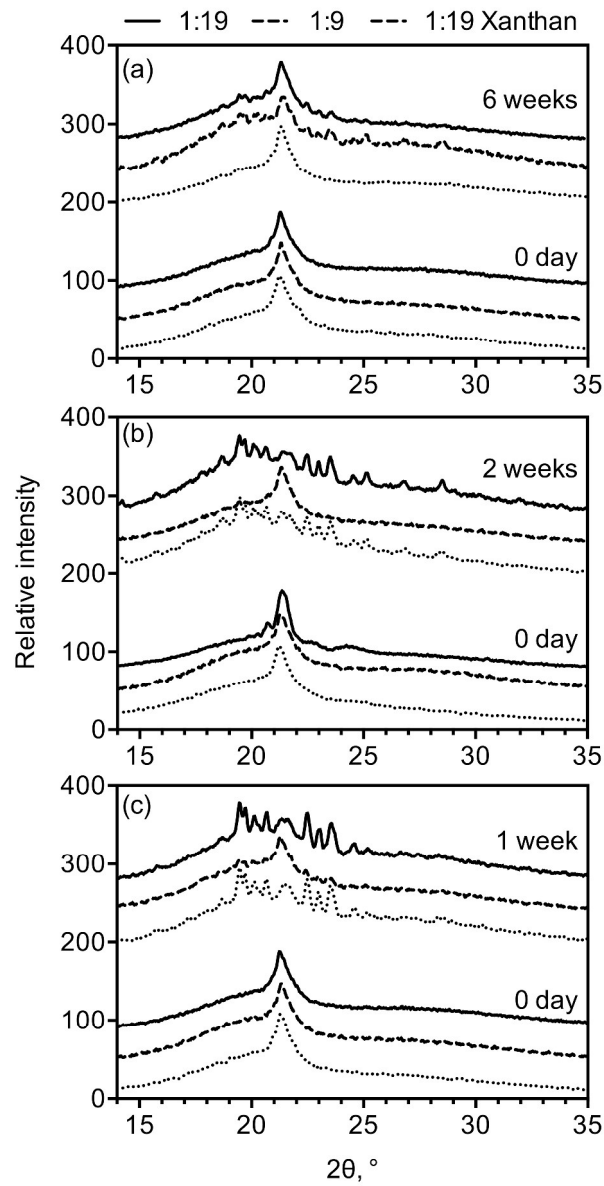
49x14mm (600 x 600 DPI)



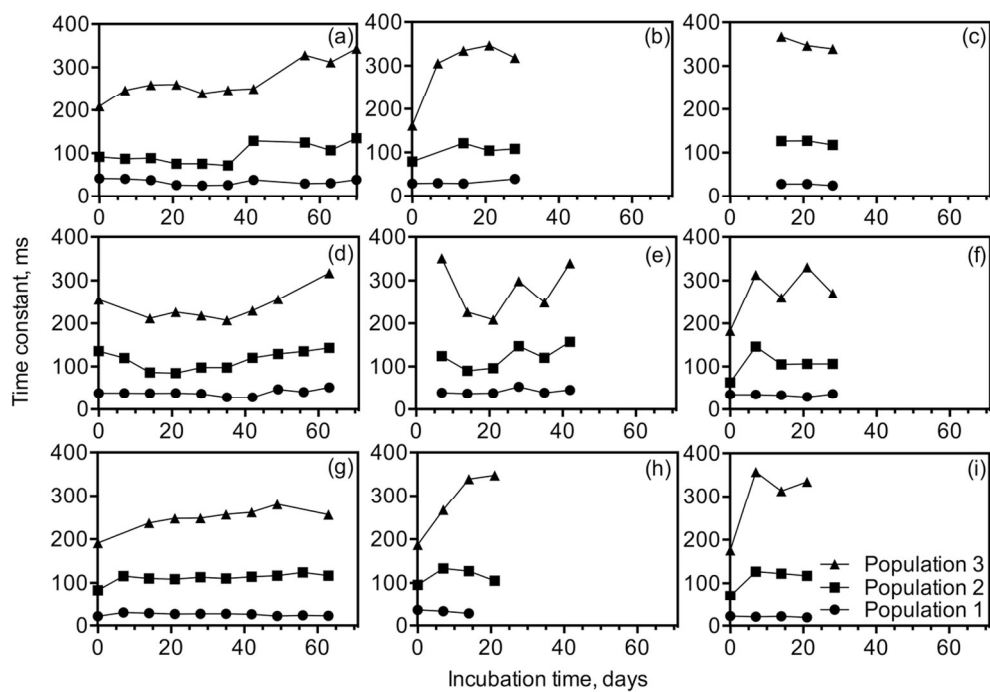
102x60mm (600 x 600 DPI)



157x297mm (600 x 600 DPI)



161x312mm (600 x 600 DPI)



120x84mm (300 x 300 DPI)